

# Model-based Reconstruction for Single Particle Cryo-Electron Microscopy

S. V. Venkatakrishnan<sup>\*</sup>, Puneet Juneja<sup>†</sup>, Hugh O’Neill<sup>o</sup>

## Abstract

Single particle cryo-electron microscopy is a vital tool for 3D characterization of protein structures. A typical workflow involves acquiring projection images of a collection of randomly oriented particles, picking and classifying individual particle projections by orientation, and finally using the individual particle projections to reconstruct a 3D map of the electron density profile. The reconstruction is challenging because of the low signal-to-noise ratio of the data, the unknown orientation of the particles, and the sparsity of data especially when dealing with flexible proteins where there may not be sufficient data corresponding to each class to obtain an accurate reconstruction using standard algorithms. In this paper we present a model-based image reconstruction technique that uses a regularized cost function to reconstruct the 3D density map by assuming known orientations for the particles. Our method casts the reconstruction as minimizing a cost function involving a novel forward model term that accounts for the contrast transfer function of the microscope, the orientation of the particles and the center of rotation offsets. We combine the forward model term with a regularizer that enforces desirable properties in the volume to be reconstructed. Using simulated data, we demonstrate how our method can significantly improve upon the typically used approach.

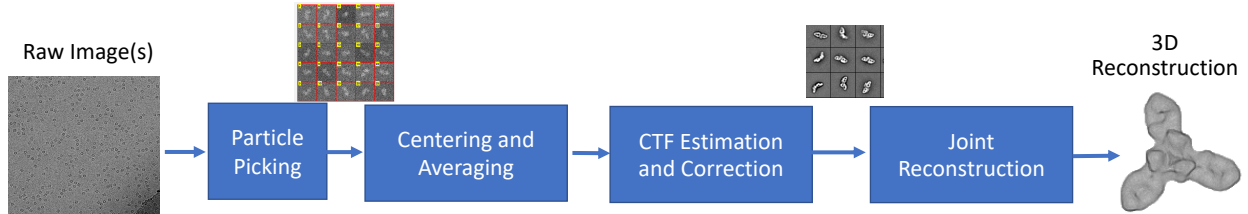


Fig. 1. Simplified illustration of the processing pipeline for SPR. The central challenge is one of reconstructing the 3D structure of an object from extremely noisy data that corresponds to the projection of the original object at certain unknown orientations.

## I. INTRODUCTION

Single particle reconstruction (SPR) for cryogenic electron microscopy (cryo-EM) involves determining the 3D structure of macro-molecules from projection images of randomly oriented replicates of these particles which are flash frozen in vitrified ice and imaged using an EM [1]. A typical reconstruction workflow (see Fig. 1) involves picking the particles from an image containing the projection of a large number of these particles, centering the picked particles, clustering and averaging similar particles to boost the SNR corresponding to a certain orientation, deconvolving these resulting images which are impacted by the contrast transfer function of the microscope (CTF correction), followed by an iterative scheme that jointly estimates the orientation and reconstructs the 3D volume [1]. Due to dose limitations, the data is extremely noisy making it challenging to obtain high-quality single particle reconstructions.

The tomographic reconstruction (for a fixed set of orientations) is often done using a direct/iterative Fourier method [2]–[4], because it is fast and hence appealing to use in an iterative refinement procedure. However, such methods can result in severe artifacts in the presence of noise and the absence of a uniform sampling of projection orientations because of the preferential

\* Multi-modal Sensor Analytics Group, Oak Ridge National Laboratory, Oak Ridge, TN 37831, USA

† Iowa State University, Ames, IA 50011, USA

° Neutron Scattering Division, Oak Ridge National Laboratory, Oak Ridge, TN 37831, USA

This abstract has been authored by UT-Battelle, LLC., under Contract No. DE-AC05-00OR22725 with the U.S. Department of Energy. The United States Government and the publisher, by accepting the article for publication, acknowledges that the United States Government retains a non-exclusive, paid-up, irrevocable, world-wide license to publish or reproduce the published form of this manuscript, or allow others to do so, for United States Government purposes. DOE will provide public access to these results of federally sponsored research in accordance with the DOE Public Access Plan (<http://energy.gov/downloads/doe-public-access-plan>).

orientation of particles [5]. Furthermore, there is increasing interest to study flexible protein structures [6], which consist of particles from different conformations in the data resulting in fewer overall orientations and more noise when particles are averaged. Finally, even if the standard methods are used to reconstruct a particle, the reconstructions can be significantly improved with a final reconstruction step that uses the estimated orientation with the *raw noisy measurements* to obtain a reconstruction using a more advanced method than the direct Fourier techniques as has been demonstrated in a wide variety of electron tomography applications [7]–[9].

While direct or iterative Fourier methods are predominantly used for SPR [2]–[4], a few model-based/regularized iterative methods have been proposed to improve the reconstruction step. These methods solve the reconstruction by minimizing a cost function that balances a data-fidelity term based on a forward model and a regularization term based on some assumptions about the underlying object itself. Liu et al. [10] presented a reconstruction algorithm (for known particle orientations) by using a quadratic data-fitting term along with a total-variation regularizer applied to coefficients in spline-basis. However, this work does not take into account the contrast transfer function of the microscope and the offset of the particles with respect to the center of the projections in the forward model. Kuckukelbir et al. [11] used an adaptive wavelet basis along with a  $l_1$  regularizer on the coefficients to illustrate how the reconstruction can be improved compared to traditional methods. Pan et al. [12] solve the reconstruction using a total-variation prior, while Donati et al. [13], [14] formulate a regularized cost function using a spline basis that allows for fast multi-scale reconstruction. Zehni et al. [15] developed a regularized iterative reconstruction technique that also takes into account the joint-estimation of the angles in addition to the 3D reconstruction by using a radial-basis function to parameterize the volume and a total-variation regularizer for the coefficients. In summary, there have been a few efforts at leveraging the success of model-based/regularized iterative techniques to improve single particle reconstructions.

In this paper, we present a model-based image reconstruction (MBIR) approach based on minimizing a regularized cost function [8] for solving the single particle cryo-EM problem *for a known set of particle orientations*. This method can be used within a refinement loop or applied as a final step to the raw measurements in order to obtain a high quality reconstruction from noisy, and limited orientation data sets. In contrast to the methods in [10], [12], [13] that rely on

a spline basis, we use a simple voxel basis with projectors implemented to work with graphic processing units (GPU). Our forward projectors includes a model for center-of-rotation offsets and the contrast transfer function of the microscope, thereby avoiding the need to pre-process the data which can result in a loss of resolution. Furthermore, the proposed forward model also allows for modeling of non Gaussian noise in the data; which is more accurate for the extremely low SNR count data that is encountered in cryo-EM detectors. Furthermore, instead of restricting ourselves to a  $l_1$  or TV regularizer [10]–[13], [15], we use a generalized Markov random field [16] based regularizer allowing for a broader range of solutions. We demonstrate the utility of our algorithm on realistic simulated data sets and highlight the utility of the method compared to the pre-process and reconstruct approach of Fig. 1.

## II. MODEL-BASED IMAGE RECONSTRUCTION

In order to reconstruct the density in 3D, we use the MBIR [17] framework. The reconstruction is formulated as a minimization problem,

$$\hat{f} \leftarrow \underset{f}{\operatorname{argmin}} \{l(g; f) + s(f)\} \quad (1)$$

where  $g$  is the vector of projection measurements,  $f$  is the vector containing all the voxels,  $l(\cdot)$  is a data fidelity enforcing function and  $s(\cdot)$  is a function that enforces regularity in  $f$ . To formulate the data fidelity term, we use the physics-based model (see Fig. 2) where each measured image is modeled as the projection of the unknown object at a specific orientation and offset, followed by a propagation effect due to the contrast transfer function of the microscope. Since the measurements are typically corrupted by noise that depends on the acquisition dose, we propose a quadratic data-fidelity term of the form

$$l(g; f) = \frac{1}{2} \|g - H A f\|_W^2 \quad (2)$$

where  $H$  is a matrix modeling the contrast transfer function (CTF) of the imaging system as a linear shift invariant filter,  $A$  is a forward projection matrix that accounts for the 3D orientation ( $\Theta_i$ ) of the particles and offsets ( $t_i$ ) of the projections from the center of the projection images, and  $W$  is a diagonal matrix with entries set to be the inverse variance of the noise in  $g$  (“dose weighting”). The  $W$  matrix can also be used to mask regions of the measurements that are corrupted due to various other reasons (like overlapping particles), providing an additional

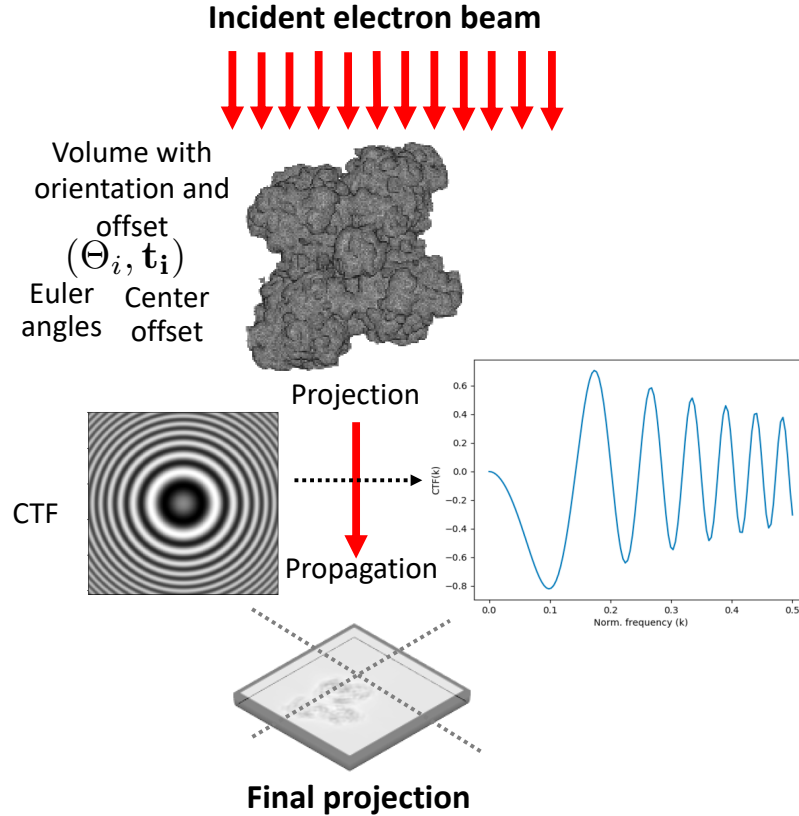


Fig. 2. Illustration of the forward model used for the cryo-EM MBIR method. It involves a 3D projection at a fixed orientation (with appropriate offset for the center of rotation) followed by a propagation operator that depends on the contrast transfer function (CTF) of the system. The figure shows an example of the magnitude of the Fourier transform of a typical CTF, illustrating that the CTF typically *zeros out* several frequency components of the projection data. While this can pose challenges for typical pre-process and reconstruct approaches, we use this model in order to perform the reconstruction.

flexibility to the reconstruction. Notice, that in contrast to existing approaches which apply “centering” and “CTF correction” to the data, our approach models these into the reconstruction itself. Furthermore, if the data sets contains measurements made at multiple defocus values corresponding to different CTFs, this can be simply incorporated in the model described above. We design  $A$  to model the cryo-EM geometry by using the ASTRA tool-box [18], [19] that can utilize multiple GPUs [20], [21] to accelerate the application of this matrix. We note that despite the projection ( $A$ ) and back-projection operators ( $A^T$ ) not being perfectly matched in ASTRA, we did not observe any specific problems with convergence of the overall algorithm. The CTF

is assumed to be radially symmetric and is modeled as

$$h(k) = \exp\{-\alpha k\} \sin\left(-\pi\Delta z \lambda k^2 + \frac{\pi}{2} C_s \lambda^3 k^4\right) \quad (3)$$

where  $k$  is the radial frequency component,  $\alpha$  is an attenuation coefficient,  $\Delta z$  is the defocus,  $\lambda$  is the electron wavelength, and  $C_s$  is the spherical aberration.

For  $s(f)$ , we choose the negative log of q-generalized Markov-random field (qGGMRF) probability density function [16]. It is given by

$$s(f) = \sum_{\{j,k\} \in \mathcal{N}} w_{jk} \rho(f_j - f_k)$$

$$\rho(f_j - f_k) = \frac{\left|\frac{f_j - f_k}{\sigma_f}\right|^2}{c + \left|\frac{f_j - f_k}{\sigma_f}\right|^{2-p}}$$

$\mathcal{N}$  is the set of pairs of neighboring voxels (e.g. a 26 point neighborhood),  $1 \leq p \leq 2$ ,  $c$  and  $\sigma_f$  are qGGMRF parameters. The weights  $w_{jk}$  are inversely proportional to the distance between voxels  $j$  and  $k$ , normalized to 1. This model provides a greater degree of flexibility in the quality of reconstructions compared to an algorithm specifically designed for a total-variation regularizer that may force the reconstructions to appear ‘‘waxy’’ [17]. In particular, when  $p = 1$  we get a behavior similar to a total-variation model and when  $p = 2$  the regularizer is a quadratic function allowing for smoother reconstructions.

Combining the data fidelity model (2) with the image model (4) the MBIR cost function is

$$c(f) = \frac{1}{2} \|g - H A f\|_W^2 + s(f) \quad (4)$$

Thus, the reconstruction is obtained by

$$\hat{f} \leftarrow \underset{f}{\operatorname{argmin}} c(f)$$

We use the optimized gradient method (OGM) [22] to find a minimum of the cost function. The algorithm involves a standard gradient computation combined with a step-size determined

using Nesterov’s method. Specifically, for each iteration  $k$ ,

$$h^{(k+1)} \leftarrow f^{(k)} - \frac{1}{L} \nabla c(f^{(k)}) \quad (5)$$

$$t^{(k+1)} \leftarrow \frac{1 + \sqrt{1 + 4(t^{(k)})^2}}{2} \quad (6)$$

$$f^{(k+1)} \leftarrow h^{(k+1)} + \frac{t^{(k)} - 1}{t^{(k+1)}} (h^{(k+1)} - h^{(k)}) \quad (7)$$

$$+ \frac{t^{(k)}}{t^{(k+1)}} (h^{(k+1)} - f^{(k)}) \quad (8)$$

where  $t^{(0)} = 1$ ,  $L$  is the Lipschitz constant of the gradient of  $c(\cdot)$ ,  $h^{(0)} = f^{(0)}$  is an initial estimate for the reconstruction. The gradient of the cost-function  $c(\cdot)$  is given by

$$\nabla c(f) = -H^T A^T W(y - H A f) + \nabla s(f). \quad (9)$$

We use the ASTRA tool-box [18], [19] to implement GPU accelerated forward and back-projection operators. For the CTF ( $H$ ) we assume circular boundary conditions and use the FFT to accelerate the computation.

### III. RESULTS

In order to evaluate our algorithm, we used three structures from the EM data bank (EMD) [23] numbered 0256 [24], 5995 [25] and 7956 [26] to generate realistic simulated cryo-EM data sets at different noise levels and a fixed sparse number of orientations (see Fig.3). In each case we applied the threshold recommended in the EMD, normalized the values by a constant and then simulated the projection measurements. The volume obtained by applying the threshold and scaling serves as the ground-truth in our experiments. The CTF parameters (equation (3)) were set to  $\alpha = 1.0$ ,  $\Delta z \lambda = 100$  and  $C_s \lambda^3 = 10$ . The orientation parameters  $\Theta$  were chosen so that each of the Euler angles were uniformly distributed in the  $[0, 2\pi]$  range leading to a preferential orientation of particles. The offset parameters  $t$  were chosen to be randomly distributed in a range of  $[0, .05 * p_w]$ , where  $p_w$  is the projected width of the simulated data in units of pixels. We simulated three different noise levels corresponding to a peak signal to noise ratio of 0 dB, 2.4dB and 6.02 dB. The number of simulated projection was set to 2 times the side length of each projection image (so if the size was  $100 \times 100$ , we simulated 200 particles). We compared the proposed algorithm to an implementation of an pre-process+reconstruct (P+R) approach where we applied a Gaussian low-pass filter to the simulated data, followed by a

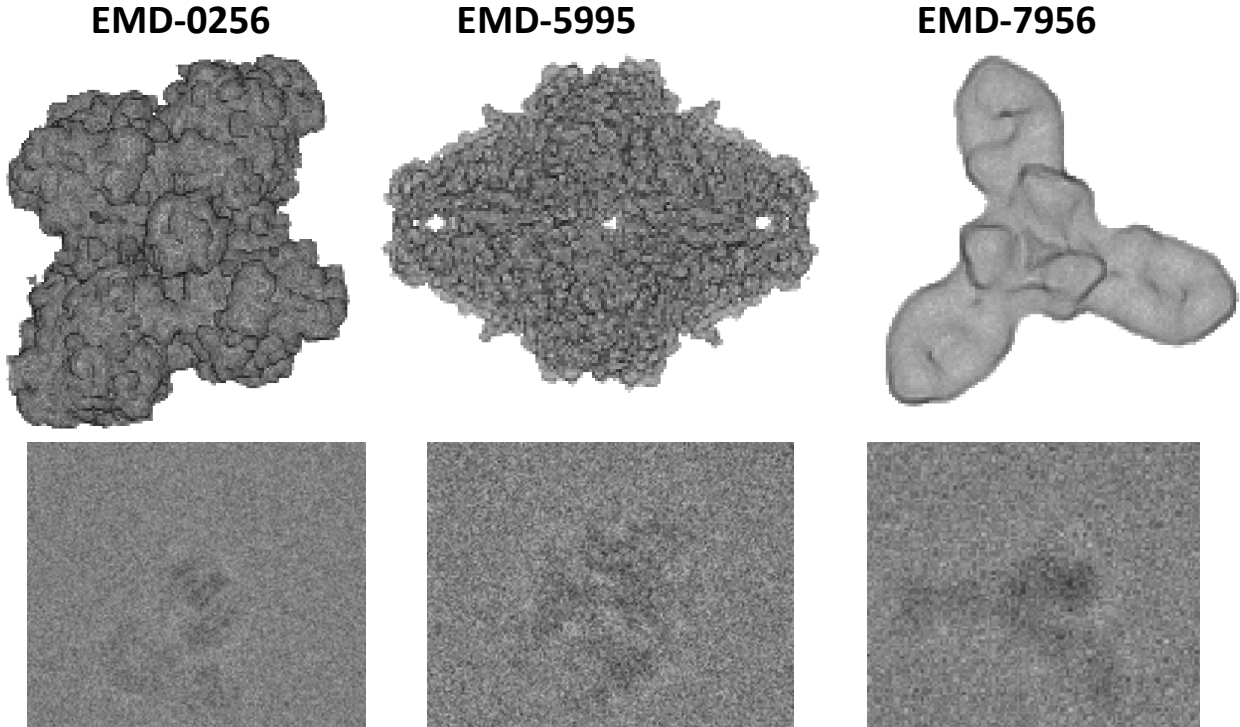


Fig. 3. 3D rendering of reference structures from the EM data bank used (top row) for generating the simulated data sets along with an example projection data (bottom row) at a peak signal-to-noise ratio of 6.02 dB.

phase-flipping technique [27] to correct for the effects of the CTF and finally reconstructing the volume using a standard least-squares type fitting technique which is a superior technique to the direct Fourier inversion techniques typically used. In each case we adjusted the algorithm parameters to determine the values that resulted in the lowest root mean squared error (RMSE).

Fig. 4 shows the results from a single cross section of the different reconstructions on the simulated data-sets at a noise level of 6.02 dB. Notice that the MBIR method can significantly improve the qualitative performance of the reconstructions compared to the P+R approach. We observe similar trends for the higher noise cases, but with an expected degradation of performance for all approaches. In order to quantify the performance of the proposed approach we present the normalized root mean squared (NRMSE) error for each of the cases (see Table. I) illustrating the significant improvements of the MBIR method compared to the P+R approach. We also perform the reconstructions by further sub-sampling the data set by selecting 50% and 25% of the original projection data and observe that the MBIR approach continues to have a lower

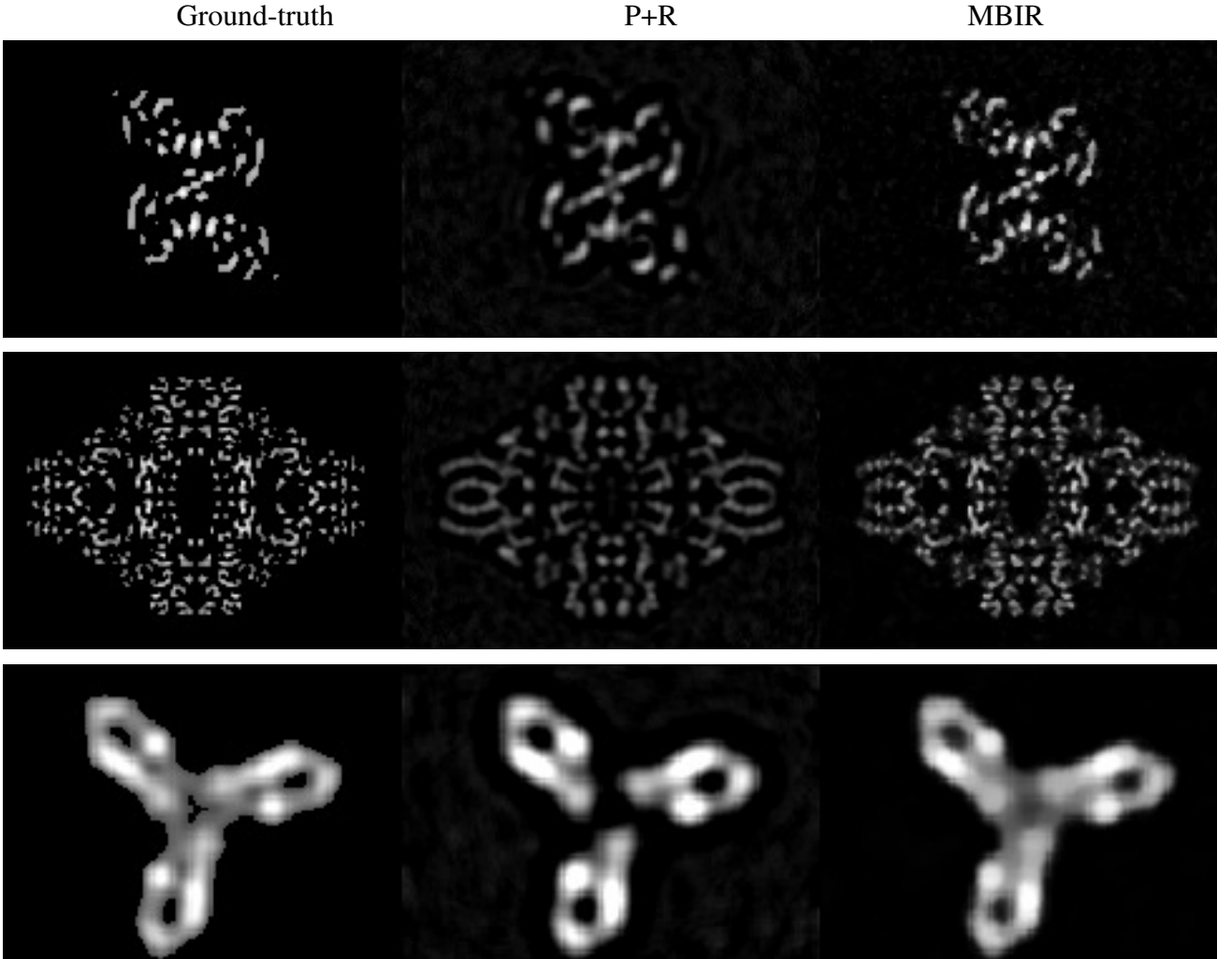


Fig. 4. A single cross section from the 3D reconstructions using different algorithms for data sets corresponding to a PSNR of 6.02 dB (Top row: EMD-0256, Middle: EMD-5995, Bottom: EMD-7956). Notice that despite a very sparse data set, the proposed MBIR method can significantly improve upon the pre-process and reconstruct (P+R) approach where the reconstruction is done using a conventional algorithm.

NRMSE compared to the P+R approach (see Table. I), highlighting that the presented approach can be very useful for cases when we have only a small number of particles to reconstruct from.

#### IV. CONCLUSION

In this paper, we presented a new model-based algorithm for single particle cryo-EM reconstruction. In contrast to existing techniques, our method casts the the reconstruction as minimizing

TABLE I

COMPARISON OF NORMALIZED ROOT MEAN SQUARE ERROR (AS PERCENTAGE OF MAX. DENSITY) FOR DIFFERENT RECONSTRUCTION SCHEMES AND DATA SETS IDENTIFIED BY THEIR EM DATA BANK (EMD) IDENTITY NUMBER AND SIMULATED NOISE LEVELS.

All projections			
Inp. PSNR	6.02 dB	2.40 dB	0 dB
EMD #	P+R MBIR	P+R MBIR	P+R MBIR
0256	6.65  <b>3.76</b>	6.76  <b>4.08</b>	6.88  <b>4.47</b>
5995	6.44  <b>4.04</b>	6.55  <b>4.50</b>	6.88  <b>4.47</b>
7956	4.65  <b>1.41</b>	4.82  <b>1.55</b>	5.03  <b>1.79</b>

50% of projections			
Inp. PSNR	6.02 dB	2.40 dB	0 dB
EMD #	P+R MBIR	P+R MBIR	P+R MBIR
0256	6.76  <b>4.08</b>	6.94  <b>4.88</b>	7.12  <b>5.13</b>
5995	6.55  <b>4.70</b>	6.94  <b>4.88</b>	7.12  <b>5.13</b>
7956	4.81  <b>1.63</b>	5.11  <b>1.73</b>	5.43  <b>1.90</b>

25% of projections			
Inp. PSNR	6.02 dB	2.40 dB	0 dB
EMD #	P+R MBIR	P+R MBIR	P+R MBIR
0256	6.94  <b>4.71</b>	7.22  <b>5.49</b>	7.48  <b>5.77</b>
5995	6.69  <b>5.21</b>	6.85  <b>5.85</b>	6.98  <b>6.17</b>
7956	5.11  <b>1.88</b>	5.56  <b>2.17</b>	5.98  <b>2.32</b>

a cost function that balances a data-fidelity term and a regularizer. We introduced a new data-fidelity term that models the contrast-transfer function, the shift in center of rotation, the 3D tomographic projection geometry, and the noise in the data in order to accurately model the cryo-EM measurement. Combining this with a standard Markov-random field based regularizer, we then developed an optimization algorithm based on first-order methods to find a minimum of the formulated cost function. Using experiments from realistic simulated data sets, we demonstrated that our algorithm can dramatically improve reconstruction quality compared to traditional pre-process and reconstruct approach.

## V. ACKNOWLEDGEMENT

S.V. Venkatakrishnan and Hugh O’Neill were supported by Oak Ridge National Laboratory via the LDRD program.

## REFERENCES

- [1] Fred J Sigworth, “Principles of cryo-EM single-particle image processing,” *Microscopy*, vol. 65, no. 1, pp. 57–67, 2016.
- [2] Pawel A Penczek, Robert Renka, and Hermann Schomburg, “Gridding-based direct fourier inversion of the three-dimensional ray transform,” *JOSA A*, vol. 21, no. 4, pp. 499–509, 2004.
- [3] Lanhui Wang, Yoel Shkolnisky, and Amit Singer, “A fourier-based approach for iterative 3D reconstruction from cryo-EM images,” *arXiv preprint arXiv:1307.5824*, 2013.
- [4] V Abrishami, JR Bilbao-Castro, J Vargas, R Marabini, JM Carazo, and COS Sorzano, “A fast iterative convolution weighting approach for gridding-based direct fourier three-dimensional reconstruction with correction for the contrast transfer function,” *Ultramicroscopy*, vol. 157, pp. 79–87, 2015.
- [5] Philip R Baldwin and Dmitry Lyumkis, “Non-uniformity of projection distributions attenuates resolution in cryo-EM,” *BioRxiv*, p. 635938, 2019.
- [6] Seth A Villarreal and Phoebe L Stewart, “CryoEM and image sorting for flexible protein/DNA complexes,” *Journal of structural biology*, vol. 187, no. 1, pp. 76–83, 2014.
- [7] S. Venkatakrishnan, L.F. Drummy, M. Jackson, M. De Graef, J. Simmons, and C.A. Bouman, “A model based iterative reconstruction algorithm for high angle annular dark field - scanning transmission electron microscope (HAADF-STEM) tomography,” *IEEE Trans. on Image Processing*, vol. 22, no. 11, Nov. 2013.
- [8] S. Venkatakrishnan, L.F. Drummy, M. Jackson, M. De Graef, J. Simmons, and C.A. Bouman, “Model based iterative reconstruction for bright-field electron tomography,” *IEEE Trans. on Computational Imaging*, vol. 1, no. 1, pp. 1–15, March 2015.
- [9] Rui Yan, Singanallur V Venkatakrishnan, Jun Liu, Charles A Bouman, and Wen Jiang, “MBIR: A cryo-ET 3D reconstruction method that effectively minimizes missing wedge artifacts and restores missing information,” *Journal of structural biology*, vol. 206, no. 2, pp. 183–192, 2019.
- [10] Ming Li, Guoliang Xu, Carlos OS Sorzano, Fei Sun, and Chandrajit L Bajaj, “Single-particle reconstruction using L2-gradient flow,” *Journal of structural biology*, vol. 176, no. 3, pp. 259–267, 2011.
- [11] Alp Kucukelbir, Fred J Sigworth, and Hemant D Tagare, “A Bayesian adaptive basis algorithm for single particle reconstruction,” *Journal of structural biology*, vol. 179, no. 1, pp. 56–67, 2012.
- [12] Huan Pan, You Wei-Wen, and Tiejong Zeng, “A fast iterative shrinkage thresholding algorithm for single particle reconstruction of cryo-EM,” in *2018 IEEE 3rd International Conference on Image, Vision and Computing (ICIVC)*. IEEE, 2018, pp. 342–346.
- [13] Laurène Donati, Masih Nilchian, Carlos Oscar S Sorzano, and Michael Unser, “Fast multiscale reconstruction for Cryo-EM,” *Journal of structural biology*, vol. 204, no. 3, pp. 543–554, 2018.
- [14] Laurène Donati, Emmanuel Soubies, and Michael Unser, “Inner-loop free ADMM for Cryo-EM,” in *ISBI 2019-IEEE International Symposium on Biomedical Imaging*, 2019.
- [15] Mona Zehni, Laurène Donati, Emmanuel Soubies, Zhizhen J Zhao, and Michael Unser, “Joint angular refinement and reconstruction for single-particle cryo-EM,” *IEEE Transactions on Image Processing*, 2020.

- [16] Jean-Baptiste Thibault, K. Sauer, C. Bouman, and J. Hsieh, “A three-dimensional statistical approach to improved image quality for multislice helical CT,” *Med. Phys.*, vol. 34, pp. 4526–4544, 2007.
- [17] Charles A. Bouman, *Model Based Image Processing*, 2013.
- [18] W.J. Palenstijn, K.J. Batenburg, and J. Sijbers, “Performance improvements for iterative electron tomography reconstruction using graphics processing units (GPUs),” *Journal of Structural Biology*, vol. 176, no. 2, pp. 250 – 253, 2011.
- [19] Wim van Aarle, Willem Jan Palenstijn, Jan De Beenhouwer, Thomas Altantzis, Sara Bals, K. Joost Batenburg, and Jan Sijbers, “The ASTRA toolbox: A platform for advanced algorithm development in electron tomography,” *Ultramicroscopy*, vol. 157, no. Supplement C, pp. 35 – 47, 2015.
- [20] Wim van Aarle, Willem Jan Palenstijn, Jeroen Cant, Eline Janssens, Folkert Bleichrodt, Andrei Dabrovolski, Jan De Beenhouwer, K. Joost Batenburg, and Jan Sijbers, “Fast and flexible X-ray tomography using the ASTRA toolbox,” *Opt. Express*, vol. 24, no. 22, pp. 25129–25147, Oct 2016.
- [21] Folkert Bleichrodt, Tristan van Leeuwen, Willem Jan Palenstijn, Wim van Aarle, Jan Sijbers, and K. Joost Batenburg, “Easy implementation of advanced tomography algorithms using the ASTRA toolbox with Spot operators,” *Numerical Algorithms*, vol. 71, no. 3, pp. 673–697, Mar 2016.
- [22] D. Kim and J. A. Fessler, “An optimized first-order method for image restoration,” in *2015 IEEE International Conference on Image Processing (ICIP)*, Sept 2015, pp. 3675–3679.
- [23] Catherine L Lawson, Ardan Patwardhan, Matthew L Baker, Corey Hryc, Eduardo Sanz Garcia, Brian P Hudson, Ingvar Lagerstedt, Steven J Ludtke, Grigore Pintilie, Raul Sala, et al., “EMDatabank unified data resource for 3DEM,” *Nucleic acids research*, vol. 44, no. D1, pp. D396–D403, 2015.
- [24] Konstantin M Boyko, Timur N Baymukhametov, Yury M Chesnokov, Michael Hons, Sofya V Lushchekina, Petr V Konarev, Alexey V Lipkin, Alexandre L Vasiliev, Patrick Masson, Vladimir O Popov, et al., “3D structure of the natural tetrameric form of human butyrylcholinesterase as revealed by cryoEM, SAXS and MD,” *Biochimie*, vol. 156, pp. 196–205, 2019.
- [25] Alberto Bartesaghi, Doreen Matthies, Soojay Banerjee, Alan Merk, and Sriram Subramaniam, “Structure of  $\beta$ -galactosidase at 3.2-Å resolution obtained by cryo-electron microscopy,” *Proceedings of the National Academy of Sciences*, vol. 111, no. 32, pp. 11709–11714, 2014.
- [26] Pavlo Gilchuk, Natalia Kuzmina, Philipp A Illynykh, Kai Huang, Bronwyn M Gunn, Aubrey Bryan, Edgar Davidson, Benjamin J Doranz, Hannah L Turner, Marnie L Fusco, et al., “Multifunctional pan-ebolavirus antibody recognizes a site of broad vulnerability on the ebolavirus glycoprotein,” *Immunity*, vol. 49, no. 2, pp. 363–374, 2018.
- [27] Amit Singer et al., “Mathematics for cryo-electron microscopy,” *arXiv preprint arXiv:1803.06714*, 2018.